SHORT REPORT

Atypical Diffusion Tensor Hemispheric Asymmetry in Autism

Nicholas Lange, Molly B. DuBray, Jee Eun Lee, Michael P. Froimowitz, Alyson Froehlich, Nagesh Adluru, Brad Wright, Caitlin Ravichandran, P. Thomas Fletcher, Erin D. Bigler, Andrew L. Alexander, and Janet E. Lainhart

Background: Biological measurements that distinguish individuals with autism from typically developing individuals and those with other developmental and neuropsychiatric disorders must demonstrate very high performance to have clinical value as potential imaging biomarkers. We hypothesized that further study of white matter microstructure (WMM) in the superior temporal gyrus (STG) and temporal stem (TS), two brain regions in the temporal lobe containing circuitry central to language, emotion, and social cognition, would identify a useful combination of classification features and further understand autism neuropathology. *Methods*: WMM measurements from the STG and TS were examined from 30 high-functioning males satisfying full criteria for idiopathic autism aged 7–28 years and 30 matched controls and a replication sample of 12 males with idiopathic autism and 7 matched controls who participated in a previous case–control diffusion tensor imaging (DTI) study. Language functioning, adaptive functioning, and psychotropic medication usage were also examined. *Results*: In the STG, we find reversed hemispheric asymmetry of two separable measures of directional diffusion coherence, tensor skewness, and fractional anisotropy. In autism, tensor skewness is greater on the right and fractional anisotropy is decreased on the left. We also find increased diffusion parallel to white matter fibers bilaterally. In the right not left TS, we find increased omnidirectional, parallel, and perpendicular diffusion. These six multivariate measurements possess very high ability to discriminate individuals with autism from individuals without autism with 94% sensitivity, 90% specificity, and 92% accuracy in our original and replication samples. We also report a near-significant association between the classifier and a quantitative trait index of autism and significant correlations between two classifier components and measures of language, IQ, and adaptive functioning in autism.

Keywords: adaptive functioning; classification; diffusion tensor imaging; hemispheric asymmetry; language functioning

Introduction

Objective in vivo biological measurements that distinguish individuals with autism from typically developing individuals and those with other developmental neuropsychiatric disorders must demonstrate very high classification ability to have applied clinical value and to elucidate neuropathology specific to autism. Biological measurements proposed to date are not yet clinically adequate and none has been replicated in an independent sample [Lainhart & Lange, 2011] (Table I). The pathogenesis of autism appears to involve white matter microstructure (WMM) and atypical inter-hemispheric functioning even in the absence of volumetric differences [Alexander et al., 2007; Bigler et al., 2007; Flagg, Cardy, Roberts, & Roberts, 2005; Fletcher et al., 2010; Kleinhans, Muller, Cohen, & Courchesne, 2008; Wilson, Rojas, Reite, Teale, & Rogers, 2007].

Diffusion tensor imaging (DTI) measures WMM by mapping directions of water diffusion in a local brain tissue frame of reference [Basser, Mattiello, & LeBihan, 1994]. Each tensor is a geometrically organized set of six 3D diffusion rates summarized typically by four coefficients: fractional anisotropy [FA, directional diffusion coherence along axons, Basser & Pierpaoli, 1996; Pierpaoli & Basser, 1996]; mean diffusivity (MD, omnidirectional

Additional Supporting Information may be found in the online version of this article.

From the Department of Psychiatry, Harvard Medical School, Boston, Massachusetts (N.L., M.P.F., C.R.); Department of Biostatistics, Harvard School of Public Health, Boston, Massachusetts (N.L.); Neurostatistics Laboratory, McLean Hospital, Belmont, Massachusetts (N.L., M.P.F.); Department of Psychiatry, School of Medicine, University of Utah, Salt Lake City, Utah (M.B.D., A.F., E.D.B., J.E.L.); Interdepartmental Neuroscience Program, University of Utah, Salt Lake City, Utah (M.B.D., J.E.L.); Waisman Laboratory for Brain Imaging and Behavior, University of Wisconsin, Madison, Wisconsin (N.A., A.L.A.); School of Medicine, University of Utah, Salt Lake City, Utah (B.W., J.E.L.); Laboratory for Psychiatric Biostatistics, McLean Hospital, Belmont, Massachusetts (C.R.); School of Computing, University of Utah, Salt Lake City, Utah (P.T.F.); Scientific Computing and Imaging Institute, University of Utah, Salt Lake City, Utah (P.T.F.); The Brain Institute at the University of Utah, Salt Lake City, Utah (P.T.F., E.D.B., J.E.L.); Department of Psychology, Brigham Young University, Provo, Utah (E.D.B.); Neuroscience Center, Brigham Young University, Provo, Utah (E.D.B.); Department of Medical Physics, University of Wisconsin, Madison, Wisconsin (A.L.A.); Department of Psychiatry, University of Wisconsin, Madison, Wisconsin (A.L.A.)

Received May 10, 2010; accepted for publication July 21, 2010

Address for correspondence and reprints: Nicholas Lange, McLean Hospital, 115 Mill Street, Belmont, MA 02478. E-mail: nlange@hms.harvard.edu

Grant sponsor: NIMH; Grant numbers: 080826; 084795; 60450; 62015; Grant sponsor: NINDS; Grant numbers: 34783; 1677; 2291; Grant sponsors: CIBM-University of Wisconsin, MIR-Univ. Wisconsin; NICHD; Grant number: 35476; Grant sponsors: NIH MRDDRC; NIDA; Grant number: 15879; Grant sponsor: NIH/NIDCD; Grant numbers: F31DC010143; T32DC008553.
Published online 2 December 2010 in Wiley Online Library (wileyonlinelibrary.com)
DOI: 10.1002/aur.162

Table I. Biological Classification Results in Autism Spectrum Disorders

Biological characteristics	Measurement type	Brain regions	ASD/AUT[a]	TD control[a]	Sensitivity (%)	Specificity (%)	Reference
GM and WM	Volume and area	Cerebrum, cerebellum	30 LFA, 12 HFA	32	94.7	92.3	Akshoomoff et al. [2004]
GM, WM	Volume	L fusiform gyrus, R temporal stem, and R inferior temporal gyrus	33 HFA	24	85.0	83.0	Neeley et al. [2007]
GM	Cortical thickness	40,000 region-specific locations	16 HFA	11	89.0 Accuracy		Singh et al. [2008]
WM	Size distribution	Gyral window	14 (HFA&LFA)	28	67.0	89.0	Casanova et al. [2009]
Papillary light reflex	Infra-red pupillography	–	24 ASD	43	91.7	93.0	Fan et al. [2009]
GM	Cortical thickness	33 regions by hemisphere	22 ASD	16	95.0	75.0	Jiao et al. [2009]
GM	Volume	33 regions by hemisphere	22 ASD	16	77.0	69.0	Jiao et al. [2009]
WM fibers	Shape		41 HFA	32	72.0	72.0	Adluru et al. [2009]
GM	MRI network pattern classification	Frontal, temporal, parietal, and cerebellar systems	22 ASD	22	77.0	86.0	Ecker et al. [2010]
WM	MRI network pattern classification	Frontal, temporal, parietal, and cerebellar systems	22 ASD	22	73.0	64.0	Ecker et al. [2010]
GM & WM	MRI network pattern classification	Frontal, temporal, parietal, and cerebellar systems	22 ASD	22	77.0	77.0	Ecker et al. [2010]
Auditory cortex	MEG latency delay	Superior temporal gyrus	25 ASD[b]	17	75.0	81.0	Roberts et al. [2010]
Speech acts	Vocalization analysis	–	AUT non-AUT delay vs TD		Accuracy 77.0–90.0		Xu et al. [2009]

[a]All male, except for Jiao [2009], 22 ASD (19M and 3F) and 16 TD (13M and 3F).
[b]Nineteen without language impairment and six with language impairment.

Figure 1. Example tensor skewness (TSkew) shapes over the skewness range. All shapes have the same fractional anisotropy level (FA).

diffusion); axial diffusivity (D_A, parallel diffusion); and radial diffusivity (D_R, perpendicular diffusion).

We also studied tensor skewness [Basser, 1997; Conturo, McKinstry, Akbudak, & Robinson, 1996]. Normalized tensor skewness (TSkew) was termed a ''fiber-crossing index'' in a study of Williams Syndrome [Marenco et al., 2007]. TSkew quantifies a distinct component of tensor shape not captured by FA or the other tensor coefficients. Figure 1 contains prolate versus oblate tensor shapes generated at the same FA value close to our sample mean.

Geometrically, TSkew and its hemispheric asymmetry index, which we name ''SkewX,'' quantify the degree of directional diffusion coherence (prolate tensor shape, or ''linear anisotropy'') versus the degree of diffusion in tangent directions (oblate tensor shape, or ''planar anisotropy'') [Alexander, Hasan, Kindlmann, Parker, & Tsuruda, 2000; Criscione, Humphrey, Douglas, & Hunter, 2000; Ennis & Kindlmann, 2006].

Previously, we found strong autism-control differences between tensor coefficients in the superior temporal gyrus (STG) and temporal stem (TS), two structures containing WM fibers critically involved in language and social cognition [Lee et al., 2007]. In this study, we investigated the ability of tensor coefficients in the STG and TS to correctly discriminate individuals with autism from typically developing individuals.

Methods and Materials

Participants

WMM measurements were further examined in 30 high-functioning (performance IQ (PIQ) $\geq$ 85) right-handed males meeting full criteria for autism and 30 typically developing and matched males who participated in a larger cross-sectional case–control study [Lee et al., 2007]. Autism and control participants were selected based on the closeness of individual matching on age, PIQ, handedness, and head circumference.

Diagnosis

Autism diagnosis was based on ADI-R [Lord, Rutter, & Le Couteur, 1994], ADOS-G [Lord et al., 2000], DSM-IV, and ICD-10 criteria. Exclusion criteria included patient

history, Fragile-X, karyotype or clinical indications of medical causes of autism, history of severe head injury, hypoxia–ischemia, seizures, and other neurologic disorders. Psychiatric comorbidity and medication status were not exclusion criteria for individuals with autism. Lifetime psychiatric comorbidity was identified in 53% (16/30) of our autism subjects. Of these, 56% (9) had depression, 31% (5) had attention deficit/attention deficit hyperactivity disorder, 25% (4) obsessive-compulsive disorder, and 19% (3) anxiety disorder. Sixty-three percent (19/30) of subjects with autism were taking one or more psychotropic medications at the time of testing. Of these, 89% (17) used SSRIs, 26% (5) used stimulants, 26% (5) used valproic acid, 26% (5) used neuroleptics. Controls were assessed with the ADOS-G, IQ, language, and other neuropsychological tests, and a standardized psychiatric measure [Leyfer et al., 2006] to confirm typical development. All the participants were verbal at the time of testing and spoke English as their first language.

Assessments

The Edinburgh Handedness Inventory [Oldfield, 1971] quantified handedness. Maximal occipital-frontal head circumference was measured. IQ was ascertained by the DAS or WISC-III for children and the WAIS-III for adults. The CELF-3 [Semel, Wiig, & Secord, 1995] and Vineland Scales [Sparrow, Balla, & Cicchetti, 1984] measured language and adaptive functioning. The Social Responsiveness Scale (SRS) [Constantino, Przybeck, Friesen, & Todd, 2000] quantified autistic traits. The Autism Comorbidity Interview assessed lifetime history of comorbidity and ruled out any concurrent episode of major depression [Leyfer et al., 2006].

Imaging Protocol

Brain imaging, image quality control, and regional segmentation (Fig. 2) were performed as described by Lee et al. [2007].

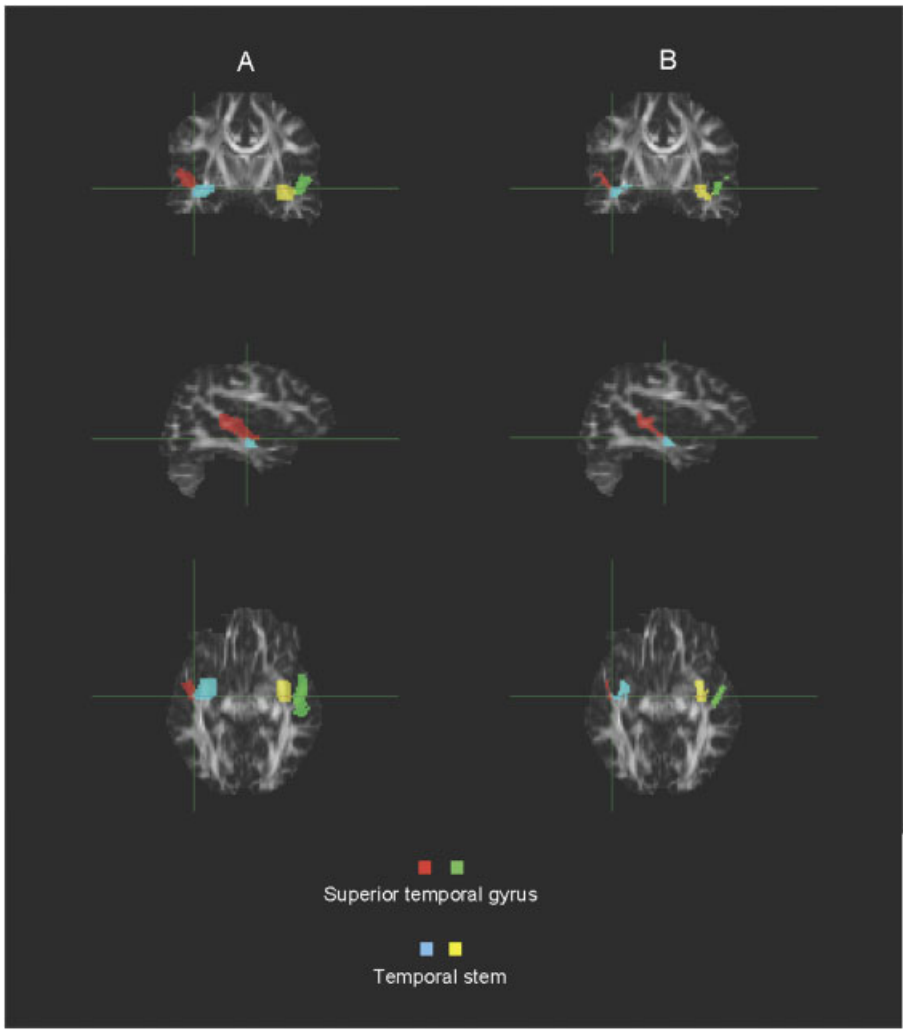

Figure 2. Example segmentation of the superior temporal gyrus and temporal stem. (**A**) Raw. (**B**) Masked for white matter only.

Biostatistics

Our focus on potential pathology in the STG and TS employs a high degree of feature selection. It provides lower exploratory power than do whole-brain approaches. We considered a maximum of six tensor coefficients to preserve at least a 10:1 subject-to-feature ratio. Each tensor coefficient was summarized by its hemispheric mean, standard deviation (SD), and coefficient of variation (CV), defined as the SD expressed as a percentage of the mean. CV is preferred to SD when comparing mean-variance pairs that may differ and may be correlated [Kennedy et al., 1998; Lange, Giedd, Castellanos, Vaituzis, & Rapoport, 1997; van Belle, Heagerty, Fisher, & Lumley, 2004], as in our sample. A hemispheric asymmetry index was defined as 2(L−R)/[L+R) [Galaburda, Corsiglia, Rosen, & Sherman, 1987], whose positive and negative values indicate leftward and rightward asymmetry. Test-wise false-positive error rate was set at 0.05 and all *P*-values were corrected by Bonferroni's method (factor of 4). We employed quadratic discriminant analysis (QDA) that included leave-one-out cross-validation and computation of Mahalanobis distances [Lange, 2005; Ripley, 1996] to identify the combination of tensor coefficients that minimized group misclassification rate. We also employed a support vector machine (SVM) [Cortes & Vapnik, 1995; Koutsouleris et al., 2009] with a Gaussian kernel and leave-one-out cross-validation to compare parametric and non-parametric approaches. Classification ability was determined by an independent 30% replication sample (12 autism and 7 control). Classification reliability was assessed by the intraclass correlation coefficient [Fleiss & Cohen, 1973]. All data analysis except the SVM was performed in R version 2.9.0.

Results

Participant Characteristics

The groups did not differ significantly with respect to age, IQ, handedness, or head circumference (Table II). As expected, the groups differed on language functioning. There was no evidence of greater subject motion in the autism sample and all image data analyzed herein passed our high-level quality control criteria [Lee et al., 2007].

Tensor Coefficients by Group, Structure, and Hemisphere

Table III contains mean, SD, and CV of the tensor coefficients. In the STG, TSkew was greater on the left in controls and greater on the right in individuals with autism ($P = 0.044$). When we accounted for statistical associations with decreased left STG FA, SkewX revealed a more significant reversal of the typical left lateralization of more prolate tensor shape in the STG (asymmetry indices: −0.0220 autism, 0.0303 control, $P = 0.0199$). TSkew and SkewX were unaffected by cross-sectional age in both groups.

Group Separation

The quadratic discriminant function identified by the first sample indicated that the combination of three tensor coefficients in the STG (SkewX, left FA and D_A bilaterally) and three in the right TS (D_A, D_R, and MD)

Table II. Physical and Cognitive Ability Characteristics of the Sample

	Control ($n = 30$)		Autism ($n = 30$)		Between-group comparison	
	Mean (SD)	Range	Mean (SD)	Range	*t* value	*P* value
Age (years)	15.79 (5.5)	8.1–26.3	15.78 (5.6)	7.0–27.8	0.10	n.s.[a]
Head Circumference[b]	56.00 (2.1)	52–59	56.63 (2.3)	53–60	1.13	n.s.
Handedness[c]	75.17 (24.9)	6–100	80.07 (22.6)	13–100	0.48	n.s.
Intelligence quotient						
Full-scale IQ	115.13 (12.9)	94–135	109.57 (16.7)	80–140	1.40	n.s.
Performance IQ	112.77 (12.5)	90–134	109.43 (13.5)	85–135	0.88	n.s.
Verbal IQ	112.80 (13.2)	90–140	106.63 (21.6)	70–145	1.34	n.s.
Language functioning[d]						
Total	109.5 (13.2)	84–137	91.34 (21.3)	50–123	3.85	<0.001
Receptive	110.0 (15.9)	82–143	93.85 (24.7)	50–125	2.76	0.008
Expressive	106.9 (12.2)	82–131	90.22 (20.0)	50–120	3.58	0.001
SRS[e]	15.9 (13.1)	0–48	99.61 (24.0)	34–148	15.93	<0.001

[a]Not statistically significant at false-positive error rate 0.05 and *P*-value greater than 0.20.
[b]Control: $n = 27$, Autism: $n = 28$.
[c]Edinburgh Handedness Inventory, range −100 (left handed) to 100 (right handed).
[d]Clinical Evaluation of Language Fundamentals (CELF-3); control: $n = 28$, Autism: $n = 30$.
[e]Social Responsiveness Scale (child) or Social Reciprocity Scale (adult), range 0 (no autistic-like traits) to 195 (many severe autistic traits). Control $n = 27$, autism $n = 28$. Verification of the 7 subjects having SRS scores less than 85 (SRS score 34, 1; 62–72, 2; 76–84, 4) confirmed that they met full diagnostic criteria for autism.

Table III. Tensor Coefficients and Asymmetry Indices by Group and Hemisphere

	Typically developing (TD) $N = 30$			Autism $N = 30$			Autism–TD		
	Left Mean (SD) CV	Right Mean (SD) CV	AI Mean (SD) CV	Left Mean (SD) CV	Right Mean (SD) CV	AI Mean (SD) CV	Left Mean (SD)	Right Mean (SD)	AI Mean (SD)
Superior temporal gyrus									
Skewness	0.517	0.502	0.0303	0.505	0.517	−0.022	−0.012	0.015	−0.0523
	(0.049)	(0.052)	(0.0969)	(0.04)	(0.049)	(0.1009)	(0.063)	(0.071)	(0.1399)
	0.095	0.103	3.1956	0.078	0.095	4.5838			
FA	0.339	0.327	0.0373	0.318	0.318	−0.0024	−0.021	−0.009	−0.0397
	(0.02)	(0.024)	(0.0529)	(0.024)	(0.018)	(0.0582)	(0.031)	(0.03)	−0.0786
	0.059	0.073	1.4182	0.075	0.057	–*			
MD (mm^2/s)	0.657	0.644	0.0194	0.671	0.661	0.0142	0.014	0.017	−0.0052
	(0.027)	(0.02)	(0.0253)	(0.027)	(0.029)	(0.0162)	(0.038)	(0.035)	(0.03)
	0.041	0.031	1.3041	0.04	0.044	1.1408			
D_A (mm^2/s)	0.9	0.87	0.0336	0.9	0.888	0.0132	0	0.018	−0.0204
	(0.035)	(0.025)	(0.038)	(0.031)	(0.035)	(0.0337)	(0.047)	(0.043)	(0.0508)
	0.039	0.029	1.131	0.034	0.039	2.553			
D_R (mm^2/s)	0.535	0.531	0.0074	0.556	0.548	0.015	0.021	0.017	0.0076
	(0.027)	(0.023)	(0.0232)	(0.03)	(0.029)	(0.0192)	(0.04)	(0.037)	(0.0301)
	0.05	0.043	3.1351	0.054	0.053	1.28			
Temporal stem									
Skewness	0.622	0.627	0.008	0.62	0.611	0.0142	−0.002	−0.016	0.0062
	(0.032)	(0.035)	(0.0644)	(0.035)	(0.032)	(0.0628)	(0.047)	(0.047)	(0.09)
	0.051	0.057	8.0024	0.057	0.052	4.4075			
FA	0.401	0.383	0.0463	0.386	0.37	0.0439	−0.015	−0.013	−0.0024
	(0.021)	(0.019)	(0.0384)	(0.019)	(0.022)	(0.044)	(0.028)	(0.029)	(0.0584)
	0.052	0.05	0.8294	0.049	0.059	1.0023			
MD (mm^2/s)	0.701	0.702	−0.0028	0.714	0.717	−0.0037	0.013	0.015	−0.0009
	(0.02)	(0.019)	(0.0177)	(0.02)	(0.023)	(0.0162)	(0.028)	(0.03)	(0.024)
	0.029	0.027	–	0.028	0.032	–			
D_A (mm^2/s)	1.018	1.001	0.0164	1.023	1.01	0.0128	0.005	0.009	−0.0036
	(0.028)	(0.02)	(0.0225)	(0.021)	(0.022)	(0.0143)	(0.035)	(0.03)	(0.0267)
	0.028	0.02	1.372	0.021	0.022	1.1172			
D_R (mm^2/s)	0.542	0.553	−0.0205	0.56	0.57	−0.0184	0.018	0.017	0.0021
	(0.022)	(0.023)	(0.0252)	(0.023)	(0.027)	(0.0272)	(0.032)	(0.035)	(0.0371)
	0.041	0.042	1.2293	0.041	0.047	1.4783			

AI, hemispheric asymmetry index 2(Left−Right)/(Left+Right), SD, standard deviation; CV, coefficient of variation; FA, fractional anisotropy; MD, mean diffusivity; D_A, axial diffusivity; D_R, radial diffusivity.
*Uninterpretable due to near-zero mean (CV < 0.01).

Table IV. Group Separation Ability of the Multivariate Collection of Diffusion Tensor Coefficients With and Without Tensor Skewness Hemispheric Asymmetry (SkewX)

	Original sample		Replication sample	
	30 autism with SkewX[a]	30 control without SkewX	12 autism with SkewX	7 control without SkewX
Sensitivity (%)	93.6	85.9	91.7	66.7
Specificity (%)	89.6	85.2	100	71.4
Accuracy (%)	91.6	85.6	94.7	68.4
PPV[b] (%)	90.0	65.6	100	80.0
NPV[c] (%)	93.3	71.5	87.5	55.6
Reliability[d] (%)	83.3	68.9	89.0	36.0

[a]Inter-hemispheric asymmetry of tensor skewness.
[b]Positive predictive value.
[c]Negative predictive value.
[d]Intraclass correlation coefficient.

Table V. A Potential DTI "Signature" for Autism

	STG	TS
Low	SkewX Left FA	–
High	D_A	Right MD Right D_A Right D_R

possessed 93.6% sensitivity, 89.6% specificity, 91.6% accuracy, 90% positive predictive value, 93.3% negative predictive value, and 83.3% reliability (Tables IV and V). The classification did not depend on cross-sectional age. Univariate dependencies of customary tensor coefficients on age were found; see Supporting Information. White matter volume was not associated with classification ability. As it is difficult without animation to visualize how all tensor coefficients combine in six dimensions,

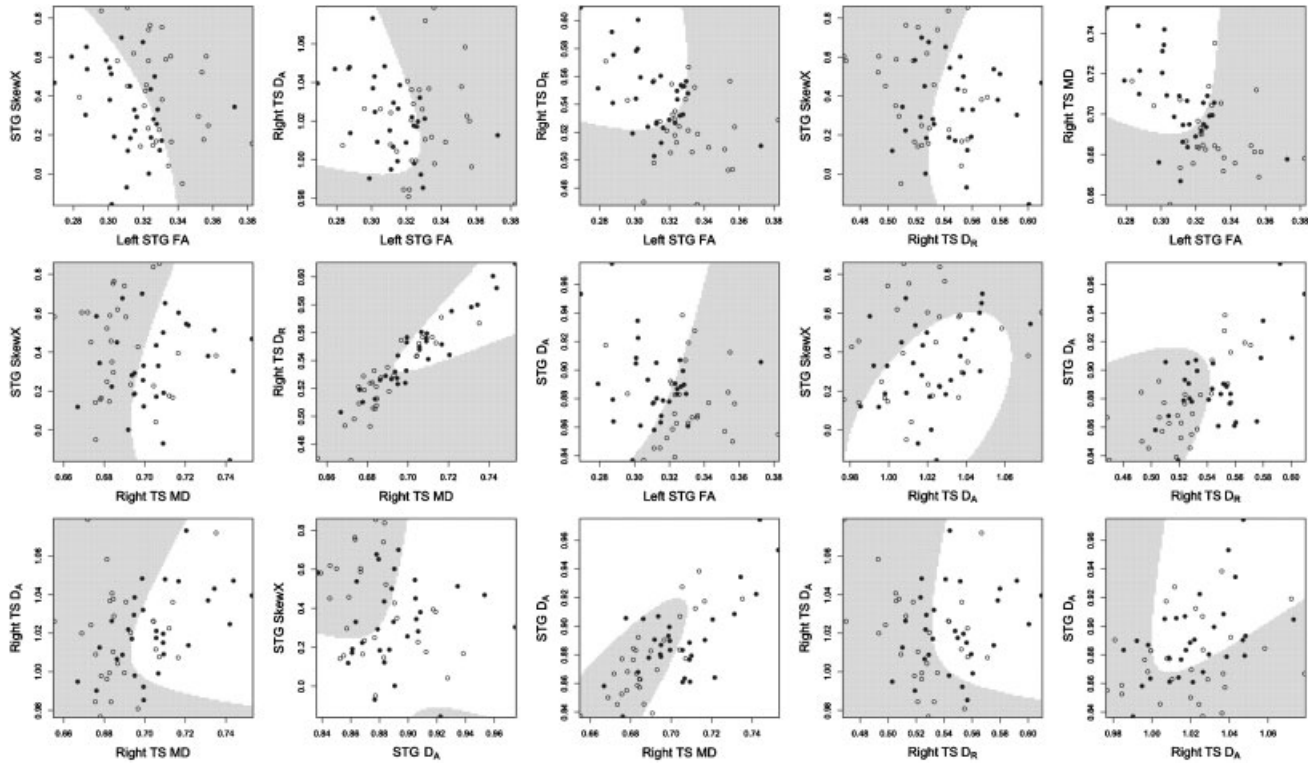

Figure 3. Bivariate plots of the six-dimensional multivariate classifier. Typically developing control values are indicated by open circles, individuals with autism by filled circles. White regions correspond to the combination of tensor coefficients that identifies an individual with autism.

bivariate plots of tensor coefficients, ordered by their decreasing rates of correct classification, provide 2D distances of individual tensor coefficients to the discrimination hyperplane (Fig. 3, left to right, top to bottom). QDA outperformed the SVM, which had lower accuracy (86.7%), positive predictive value (80.5%), and reliability (63.2%). Our comparison demonstrated the benefit of fitting a parametric model when appropriate [Altham, 1984]. Equally high performance of the QDA discrimination rule was found when applied to the independent replication sample (Table IV). Decreased STG SkewX had the largest influence of all classifier coefficients, followed by decreased left STG FA. When applied to the independent sample, a deficient algorithm without STG SkewX showed much poorer performance (Table IV).

Clinical Correlation

The distances of individual sets of all six tensor coefficients to the classifier boundary were correlated with individual SRS scores, but did not reach statistical significance ($P = 0.08$, uncorrected). Low leftward FA in the STG was associated with the composite Vineland score ($P = 0.004$, uncorrected; $P = 0.024$, corrected) and high rightward perpendicular diffusion in the TS was correlated with the CELF-3 Receptive score ($P = 0.018$, uncorrected) and with PIQ ($P = 0.035$, uncorrected).

Discussion

Our observations suggest a greater disruption of spatial organization of STG and TS white matter fibers in autism than what has been reported previously. The principal new findings of this study are reversed hemispheric asymmetry of diffusion tensor skewness in the STG in autism and very high ability of the physical properties of white matter microstructure (WMM) in the STG and TS to separate individuals with autism from typically developing individuals. Skewness characterizes the shape of the diffusion tensor, a component of the directional coherence of water diffusion in white matter not captured by FA. The multivariate composition of six tensor coefficients illuminates the differences in tensor skewness hemispheric asymmetry and other WMM diffusion tensor coefficients in the STG and TS that best distinguish individuals with autism from typically developing individuals.

We have no evidence that non-autistic factors account for the observed findings. Image quality was equally high in both groups. A few younger participants with autism were sedated for scanning but the group separation method performed equally well in younger and older individuals. Some autism participants had neuropsychiatric conditions in addition to autism and were taking psychotropic medications. Our results to date suggest that, in autism, psychotropic medication usage does not affect

WMM [Alexander et al., 2007; Lee et al., 2007]. The nearly significant correlation of the multivariate combination of six tensor coefficients with a quantitative trait index of autism together with significant univariate associations between tensor coefficients and measures of language, IQ, and adaptive functioning provide evidence that our findings are due to autism-related differences in WMM.

Our observations have neurobiological implications. The results provide new evidence of key involvement of the STG and TS in the neurobiology of autism [Bigler et al., 2003, 2007; Lee et al., 2007, 2009; Neeley et al., 2007]. Involvement of the STG and TS indicates atypicality in both superficial and deep white matter compartments. Hemispheric reversal of tensor shape in the STG (SkewX) is the most salient atypicality, followed by a loss of typical leftward asymmetry of STG FA. These reversals suggest that directional diffusion along white matter fibers in the STG is more coherent on the right and less coherent on the left in autism and a possible disruption of factors that affect hemispheric lateralization of WMM during development. Atypicality of different tensor coefficients in the STG and the TS suggests heterogeneity of WMM changes in autism. Clinical heterogeneity in autism may be due to neuropathological heterogeneity. Atypical increases of omnidirectional and perpendicular diffusion in the right TS may be due to differences in crossing fibers, dysmyelination, fiber packing, axonal diameter, intracellular viscosity, osmotic pressure, and/or neurofibrils [Alexander et al., 2007; Beaulieu & Allen, 1994; Song et al., 2002]. Some or all of these factors could be affected in autism and be ruled in or out by advanced imaging techniques and longitudinal data. Transposition of WMM architecture as measured by SkewX in the left and right STG in the context of increased multi-component diffusion in the right TS suggest complex interactions between superficial and deep WM compartment circuitry. The TS contains important afferent and efferent fibers connecting the STG and other temporal lobe regions to the thalamus, homotopic regions in the contralateral hemisphere, and other regions in ipsilateral and contralateral hemispheres. Interactions between STG and TS circuitry may be related to atypical structure–function relationships in the STG [Bigler et al., 2007] and physiological dysfunction in subregions of the STG such as the auditory cortex [Roberts et al., 2010].

A multivariate combination of six measures of atypical deviations of WMM in the STG and right TS discriminated between individuals with autism and typically developing individuals with 94% sensitivity, 90% specificity, and 92% accuracy. Equally high performance was seen in a small independent replication sample. Our results demonstrate the ability of multivariate analysis of WMM to elide the artificial separation of biological factors adopted by univariate approaches and to provide a more comprehensive albeit clinically complex interpretation of the subtle facets of atypical brain circuitry found in autism. Future investigations that strike a scientifically effective balance between whole-brain exploratory approaches and a priori feature selection may result in even higher classification ability, reliability, and predictive power.

The neuropathology of autism remains unclear. Heterogeneous and shared neuropathology could help identify the genetic etiology of the disorder. Further development and validation of our findings in longitudinal non-human animal studies and clinical settings will increase our understanding of biological mechanisms contributing to WMM atypicality that may give rise to autism.

We acknowledge the following limitations of this work. Comparison groups of individuals with developmental disorders other than high-functioning autism are needed to determine the specificity of our results to the disorder. Our classifier employs a high degree of feature selection limiting exploratory power. Extensions of our findings to high-severity individuals with autism, infants, young children, and females are unknown at present. Future studies of larger cross-sectional and longitudinal samples are essential. The regional tensor coefficients studied are ensemble averages of local tensors, which are themselves averages of thousands of axons mixed with non-myelinated tissue that blur finer anatomic distinctions. Higher-resolution DTI studies of human and non-human animals [Assaf, Blumenfeld-Katzir, Yovel, & Basser, 2008; Barazany, Basser, & Assaf, 2009] and more informative models of autism will yield further insight on relations between microscopic white matter neuropathology and clinical features and course of the disorder.

Acknowledgments

This work was funded by NIMH080826, NIMH084795, and Autism Speaks Awards 1677 and 2291 (J.E.L.); NINDS34783 and NIMH60450 (N.L.); NICHD35476, CIBM-University of Wisconsin, MIR-Univ. Wisconsin (N.A.); NIH MRDDRC, NIMH62015, and NIDA15879 (A.L.A.); NIH/NIDCD F31DC010143 (M.B.D.); and Neuroscience Training Grant NIH NIDCD T32DC008553 (Univ. Utah). The content is solely the responsibility of the authors and does not necessarily represent the official views of the NIMH, NIDA, NINDS, NICHD, NIDCD or the NIH. We express our sincere gratitude to the children, adults and families who participated in this study. The authors report no biomedical financial interests or potential conflicts of interest.

References

Adluru, N., Hinrichs, C., Chung, M.K., Lee, J.E., Singh, V., et al. (2009). Classification in DTI using shapes of white matter tracts. Conf Proc IEEE Eng Med Biol Soc, 1, 2719–2722.

Akshoomoff, N., Lord, C., Lincoln, A.J., Courchesne, R.Y., Carper, R.A., et al. (2004). Outcome classification of

preschool children with autism spectrum disorders using MRI brain measures. Journal of the American Academy of Child and Adolescent Psychiatry, 43, 349–357.

Alexander, A.L., Hasan, K., Kindlmann, G., Parker, D.L., & Tsuruda, J.S. (2000). A geometric analysis of diffusion tensor measurements of the human brain. Magnetic Resonance in Medicine, 44, 283–291.

Alexander, A.L., Lee, J.E., Lazar, M., Boudos, R., DuBray, M.B., et al. (2007). Diffusion tensor imaging of the corpus callosum in Autism. Neuroimage, 34, 61–73.

Altham, P.M.E. (1984). Improving the precision of estimation by fitting a model. Journal of the Royal Statistical Society, Series B, 46, 118–119.

Assaf, Y., Blumenfeld-Katzir, T., Yovel, Y., & Basser, P.J. (2008). AxCaliber: A method for measuring axon diameter distribution from diffusion MRI. Magnetic Resonance in Medicine, 59, 1347–1354.

Barazany, D., Basser, P.J., & Assaf, Y. (2009). In vivo measurement of axon diameter distribution in the corpus callosum of rat brain. Brain, 132, 1210–1220.

Basser, P.J. (1997). New histological and physiological stains derived from diffusion-tensor MR images. Annals of the New York Academy of Sciences, 820, 123–138.

Basser, P.J., & Pierpaoli, C. (1996). Microstructural and physiological features of tissues elucidated by quantitative-diffusion-tensor MRI. Journal of Magnetic Resonance, Series B, 111, 209–219.

Basser, P.J., Mattiello, J., & LeBihan, D. (1994). MR diffusion tensor spectroscopy and imaging. Biophysical Journal, 66, 259–267.

Beaulieu, C., & Allen, P.S. (1994). Water diffusion in the giant axon of the squid: Implications for diffusion-weighted MRI of the nervous system. Magnetic Resonance in Medicine, 32, 579–583.

Bigler, E.D., Tate, D.F., Neeley, E.S., Wolfson, L.J., Miller, M.J., et al. (2003). Temporal lobe, autism, and macrocephaly. American Journal of Neuroradiology, 24, 2066–2076.

Bigler, E.D., Mortensen, S., Neeley, E.S., Ozonoff, S., Krasny, L., et al. (2007). Superior temporal gyrus, language function, and autism. Developmental Neuropsychology, 31, 217–238.

Casanova, M.F., El-Baz, A., Mott, M., Mannheim, G., Hassan, H., et al. (2009). Reduced gyral window and corpus callosum size in autism: Possible macroscopic correlates of a minicolumnopathy. Journal of Autism and Developmental Disorders, 39, 751–764.

Constantino, J.N., Przybeck, T., Friesen, D., & Todd, R.D. (2000). Reciprocal social behavior in children with and without pervasive developmental disorders. Journal of Developmental and Behavioral Pediatrics, 21, 2–11.

Conturo, T.E., McKinstry, R.C., Akbudak, E., & Robinson, B.H. (1996). Encoding of anisotropic diffusion with tetrahedral gradients: A general mathematical diffusion formalism and experimental results. Magnetic Resonance in Medicine, 35:399–412.

Cortes, C., & Vapnik, V. (1995). Support-vector networks. Machine Learning, 20, 273–297.

Criscione, J.C., Humphrey, J.D., Douglas, A.S., & Hunter, W.C. (2000). An invariant basis for natural strain which yields orthogonal stress response terms in isotropic hyperelasticity. Journal of the Mechanics and Physics of Solids, 48, 2445–2465.

Ecker, C., Rocha-Rego, V., Johnston, P., Mourao-Miranda, J., Marquand, A., et al. MRC AIMS Consortium. (2010). Investigating the predictive value of whole-brain structural MR scans in autism: A pattern classification approach. Neuroimage, 49, 44–56.

Ennis, D.B., & Kindlmann, G. (2006). Orthogonal tensor invariants and the analysis of diffusion tensor magnetic resonance images. Magnetic Resonance in Medicine, 55, 136–146.

Fan, X., Miles, J.H., Takahashi, N., & Yao, G. (2009). Abnormal transient pupillary light reflex in individuals with autism spectrum disorders. Journal of Autism and Developmental Disorders, 39, 1499–1508.

Flagg, E.J., Cardy, J.E., Roberts, W., & Roberts, T.P. (2005). Language lateralization development in children with autism: Insights from the late field magnetoencephalogram. Neuroscience Letters, 386, 82–87.

Fleiss, J.L., & Cohen, J. (1973). The equivalence of weighted kappa and the intraclass correlation coefficient as measures of reliability. Educational and Psychological Measurement, 33, 613–619.

Fletcher, P.T., Whitaker, R.T., Tao, R., DuBray, M.B., Froehlich, A., et al. (2010). Microstructural connectivity of the arcuate fasciculus in adolescents with high-functioning autism. Neuroimage, 51, 1117–1125.

Galaburda, A.M., Corsiglia, J., Rosen, G.D., & Sherman, G.F. (1987). Planum temporale asymmetry, reappraisal since Geschwind and Levitsky. Neuropsychologia, 25, 853–868.

Jiao, Y., Chen, R., Ke, X., Chu, K., Lu, Z., & Herskovits, E.H. (2010). Predictive models of autism spectrum disorder based on brain regional cortical thickness. Neuroimage, 50, 589–599.

Kennedy, D.N., Lange, N., Makris, N., Bates, J., Meyer, J., & Caviness, V.S.J. (1998). Gyri of the human neocortex: An MRI-based analysis of volume and variance. Cerebral Cortex, 8, 371–384.

Kleinhans, N.M., Muller, R.A., Cohen, D.N., & Courchesne, E. (2008). Atypical functional lateralization of language in autism spectrum disorders. Brain Research, 1221, 115–125.

Koutsouleris, N., Meisenzahl, E.M., Davatzikos, C., Bottlender, R., Frodl, T., et al. (2009). Use of neuroanatomical pattern classification to identify subjects in at-risk mental states of psychosis and predict disease transition. Archives of General Psychiatry, 66, 700–712.

Lainhart, J., & Lange, N. (2010). The biological broader autim phenotype. In: Amaral D, Dawson G, & Geschwind D, editors. Autism spectrum disorders. Oxford: Oxford University Press.

Lange, N. (2005). Pattern recognition. In: Armitage P & Colton T, editors. Encyclopedia of biostatistics, 2e. Hoboken, NJ: Wiley.

Lange, N., Giedd, J.N., Castellanos, F.X., Vaituzis, A.C., & Rapoport, J.L. (1997). Variability of human brain structure size: Ages 4–20 years. Psychiatry Research: Neuroimaging, 74, 1–12.

Lee, J.E., Bigler, E.D., Alexander, A.L., Lazar, M., DuBray, M.B., et al. (2007). Diffusion tensor imaging of white matter in the superior temporal gyrus and temporal stem in autism. Neuroscience Letters, 424, 127–132.

Lee, J.E., Chung, M.K., Lazar, M., DuBray, M.B., Kim, J., et al. (2009). A study of diffusion tensor imaging by tissue-specific, smoothing-compensated voxel-based analysis. Neuroimage, 44, 870–883.

Leyfer, O.T., Folstein, S.E., Bacalman, S., Davis, N.O., Dinh, E., et al. (2006). Comorbid psychiatric disorders in children with autism: Interview development and rates of disorders. Journal of Autism and Developmental Disorders, 36, 849–861.

Lord, C., Rutter, M., & Le Couteur, A. (1994). Autism diagnostic interview-revised: A revised version of a diagnostic interview for caregivers of individuals with possible pervasive developmental disorders. Journal of Autism and Developmental Disorders, 24, 659–685.

Lord, C., Risi, S., Lambrecht, L., Cook, Jr., E.H., Leventhal, B.L., et al. (2000). The autism diagnostic observation schedule-generic: A standard measure of social and communication deficits associated with the spectrum of autism. Journal of Autism and Developmental Disorders, 30, 205–223.

Marenco, S., Siuta, M.A., Kippenhan, J.S., Grodofsky, S., Chang, W.L., et al. (2007). Genetic contributions to white matter architecture revealed by diffusion tensor imaging in Williams syndrome. Proceedings of the National Academy of Sciences, 104, 15117–15122.

Neeley, E.S., Bigler, E.D., Krasny, L., Ozonoff, S., McMahon, W., & Lainhart, J.E. (2007). Quantitative temporal lobe differences: Autism distinguished from controls using classification and regression tree analysis. Brain and Development, 29, 389–399.

Oldfield, R.C. (1971). The assessment and analysis of handedness: The Edinburgh inventory. Neuropsychologia, 9, 97–113.

Pierpaoli, C., & Basser, P.J. (1996). Toward a quantitative assessment of diffusion anisotropy. Magnetic Resonance in Medicine, 36, 893–906.

Ripley, B.D. (1996). Pattern recognition and neural networks. New York: Cambridge University Press.

Roberts, T.P., Khan, S.Y., Rey, M., Monroe, J.F., Cannon, K., et al. (2010). MEG detection of delayed auditory evoked responses in autism spectrum disorders: Towards an imaging biomarker for autism. Autism Research, 3, 8–18.

Semel, E., Wiig, E.H., & Secord, W.A. (1995). Clinical evaluation of language fundamentals, 3e (CELF-3). San Antonio, TX: Psychological Corporation.

Singh, V., Mukherjee, L., & Chung, M.K. (2008). Cortical surface thickness as a classifier: Boosting for autism classification. Med Image Comput Comput Assist Interv, 11, 999–1007.

Song, S.K., Sun, S.W., Ramsbottom, M.J., Chang, C., Russell, J., & Cross, A.H. (2002). Dysmyelination revealed through MRI as increased radial (but unchanged axial) diffusion of water. Neuroimage, 17, 1429–1436.

Sparrow, S.S., Balla, D.A., & Cicchetti, D.V. (1984). Vineland adaptive behavior scales: Interview edition, survey form manual. Circle Pines, MN: American Guidance Service.

van Belle, G., Heagerty, P.J., Fisher, L.D., & Lumley, T.S. (2004). Biostatistics: A methodology for the health sciences. New York: Wiley.

Wilson, T.W., Rojas, D.C., Reite, M.L., Teale, P.D., & Rogers, S.J. (2007). Children and adolescents with autism exhibit reduced MEG steady-state gamma responses. Biological Psychiatry, 62, 192–197.

Xu, D., Gilkerson, J., Richards, J., Yapanel, U., & Gray, S. (2009). Child vocalization composition as discriminant information for automatic autism detection. Annual International Conference of the IEEE Engineering in Medicine and Biology Society, 1, 2518–2522.